

## Evaluation of structural operativity of two strategic buildings through Seismic Model

Dora Foti<sup>1</sup>, Nicola Ivan Giannoccaro<sup>\*2</sup>, Pierluigi Greco<sup>1</sup>, Michela Lerna<sup>1</sup>, Raffaele Paolicelli<sup>1</sup> and Vitantonio Vacca<sup>3</sup>

<sup>1</sup>Dipartimento di Scienze dell'Ingegneria Civile e dell'Architettura, Politecnico di Bari, 70126 Bari, Italy

<sup>2</sup>Dipartimento di Ingegneria dell'Innovazione, Università del Salento, 73100 Lecce, Italy

<sup>3</sup>Consiglio Nazionale delle Ricerche – Istituto di Geologia Ambientale e Geoingegneria, Roma, Italy

(Received March 25, 2020, Revised May 20, 2020, Accepted June, 10, 2020)

**Abstract.** This paper presents the experimental application of a new method for seismic vulnerability assessment of buildings recently introduced in literature, the SMAV (Seismic Model Ambient Vibration) methodology with reference to their operational limit state. The importance of this kind of evaluation arises from the civil protection necessity that some buildings, considered strategic for seismic emergency management, should retain their functionality also after a destructive earthquake. They do not suffer such damage as to compromise the operation within a framework of assessment of the overall capacity of the urban system. To this end, for the characterization of their operational vulnerability, a Structural Operational Index (IOPS) has been considered. In particular, the dynamic environmental vibrations of the two considered strategic buildings, the fire station and the town hall building of a small town in the South of Italy, have been monitored by positioning accelerometers in well-defined points. These measurements were processed through modern Operational Modal Analysis techniques (OMA) in order to identify natural frequencies and modal shapes. Once these parameters have been determined, the structural operational efficiency index of the buildings has been determined evaluating the seismic vulnerability of the strategic structures analyzed. This study aimed to develop a model to accurately predict the acceleration of structural systems during an earthquake.

**Keywords:** seismic vulnerability; operational modal analysis; equivalent linear model; structural operative index; nondestructive techniques; ambient vibrations; dynamic analysis

### 1. Introduction

In recent years the use of the Operational Modal Analysis (OMA), consisting of all those techniques addressed to modal parameter identification from output-only analysis (Peeters and De Roeck 2011, Reynders 2012, Ranieri and Fabbrocino 2014, Bru *et al.* 2015), to identify the unknown parameters of a building is becoming increasingly important as a nondestructive technique for performing accurate structural analyses and evaluating in situ the actual behavior of the structures (Foti *et al.* 2012, Foti *et al.* 2015). The knowledge of the modal characteristics of the structures is, in fact, of great utility in view of their performance assessments in the case of soliciting events such as earthquakes; recent studies (Mazza 2019a, Mazza 2019b, Mazza 2019c) have analyzed the effects of damage provoked by past earthquakes and the effects of masonry infills.

In this study, a dynamic identification application will be described, using the OMA methodology carried out with data collection in the field of two structures identified as being of strategic importance, that is, the provincial command building of the Taranto fire, detachment of

Castellaneta (TA) and the building of the Municipality of Ginosa (TA). After an investigation campaign with the application of accelerometers on the structures, through OMA techniques have been utilized to extract the modal forms, the vibration frequencies and the damping coefficients of both the buildings that have a completely different and irregular geometry and composed of different number of floors.

The data collected represent the basis for the evaluation of the Structural Operation of the buildings under study. In this regard, the structure's operating index and the seismic model will be assessed using the SMAV methodology presented in Mori and Spina (2015) and improved in Spina *et al.* (2019) with the introduction of the statistical structural serviceability index. The SMAV methodology is important, as it allows to know the state of health of the structure and how it would respond to the probability of being subjected to external seismic stresses. Therefore, it allows to evaluate the operating status of the building and the maximum displacement value of the floor or "drift", starting from the modal data. In the considered strategic building the first three experimentally identified modes have been used for determining the IOPS and the maximum drifts.

The paper is structured as follows: Section 2 contains a description of the strategic buildings, Section 3 describes the experimental tests, Section 4 describes the OMA results, Section 5 describes the SMAV results and, finally, Section 6 describes the paper's conclusions.

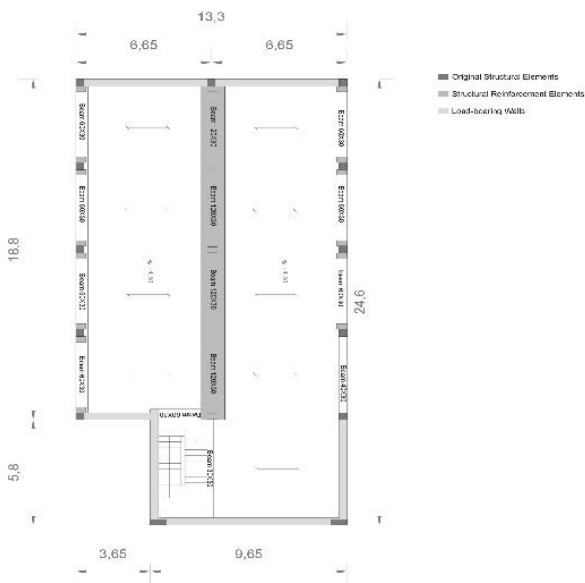
---

\*Corresponding author, Professor  
E-mail: [ivan.giannoccaro@unisalento.it](mailto:ivan.giannoccaro@unisalento.it)



Fig. 1 Fire brigade building

## STRUCTURAL PLANS Ground Floor

Fig. 2 Intermediate floor plant, quote  $z=4.5$ 

## 2. Description of the strategic buildings

### 2.1 Provincial command of the fire brigade of Castellaneta, Taranto, Italy

The first strategic building analyzed is the fire station of the Municipality of Castellaneta (depicted in Fig.1) located in the South-West area with respect to the city center, reachable by the road that connects Castellaneta to the town of Palagiano. The building has two floors above ground and consists of a frame structure in reinforced concrete and load-bearing masonry in tuff ashlars. The two levels above ground have different heights: the ground floor, hosting the garage of the fire fighters vehicles and the related workshop, has a height of about 4.5 m, while the upper floor, hosting the offices, the operations center and the rooms, has a variable height since the roof is a barrel vault in reinforced concrete with a height of 2.47 m.

The building, built in 1971, has undergone a change of intended use over the years, moving from waste storage center to fire station barracks in 1994. More in detail, due to the change of use, over the years the structure has undergone structural alterations such as the construction of

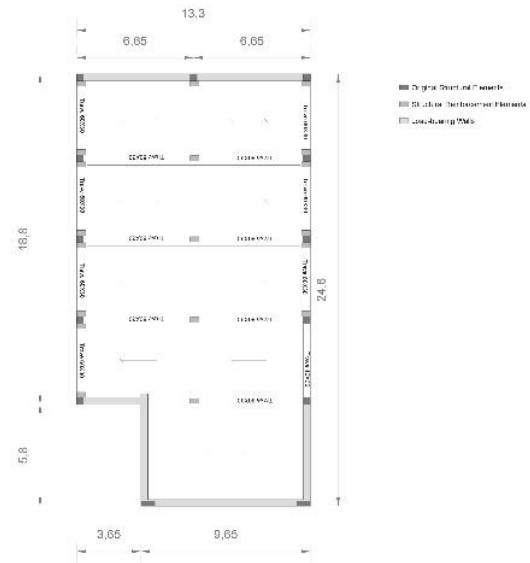
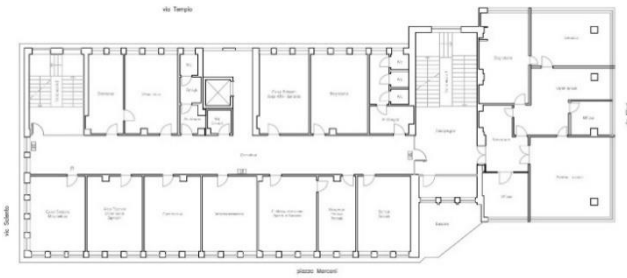
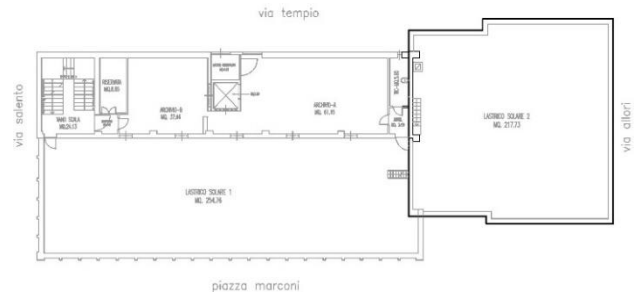
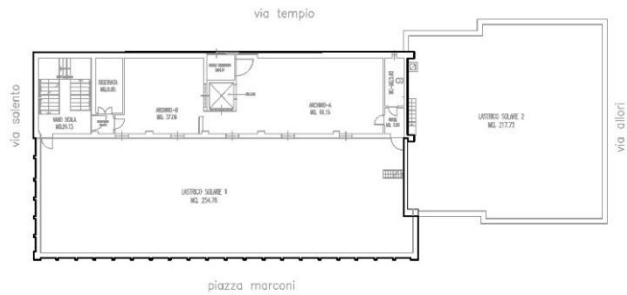
STRUCTURAL PLAN  
Roof FloorFig. 3 Coverage plant, quote  $z=12.6$  m

Fig. 4 City Hall of Ginosa

the intermediate masonry slab, in 1994, at a height of 4.5 and the construction of new pillars in 1995, connected to the original pillars, as structural reinforcement. The detailed plants with the indication of the quote  $z$ , are shown in Fig. 2 (intermediate floor) and Fig. 3 (coverage floor).

At present the structure is of a "mixed" type: most of the stresses are absorbed by the concrete frames and the reinforced concrete walls of the basement. These structures have additional supports by the load-bearing walls made of 40 cm thick tuff blocks. The floors are made up in brick-cement having a total thickness of 25 + 5 cm. Each structural element of the frame is made of reinforced concrete C25/30 and reinforcement in high adherence steel B450C. The original perimeter pillars, having a 40 × 40 cm square section, were reinforced by creating new pillars, connected to them, having a 30 × 50 cm section. In the central area of the building, on the other hand, to create the inter-floor slab, new pillars with a section of 30 × 50 cm were created connected to each other by flat beams with a section of 120 × 30 cm. Only the pillars connected to the load-bearing wall in the North elevation (short side) have a different rectangular section 30 × 80 cm. The edge beams have a 60 × 30 cm section, both for those on the first level and for those on the roof. The external claddings have an

Fig. 5 First floor plant, quote  $z=5.93$ Fig. 7 Fourth level plant, quote  $z=14.41$  mFig. 6 Third level plant, quote  $z=12.6$  mFig. 8 Fifth level plant, quote  $z=15.09$  m

irregular distribution both in plan and in height and consist of perforated brick blocks having a total thickness of about 35 cm and a surface mass of  $2.8 \text{ kN/m}^2$ . The roof of the entire building consists of a lowered arch in reinforced concrete. The levels are connected vertically by reinforced concrete stairs of the rampant type. The curtain walls have an irregular distribution in plan and height. The foundations essentially consist of connected plinths in reinforced concrete.

## 2.2 Provincial command of the fire brigade of Castellaneta, Taranto, Italy

The second analyzed strategic building is the city Hall of the town of Ginosa. It is in the North-East part of the city, close to the historical center. The building has a frame structure in reinforced concrete that rises on five different levels; the overall dimensions of the plan are approximately  $45 \times 19$  meters. The first two levels (quotes 5.93 and 9.27 m respectively) constitute the first and second floors, used for office use, the third level (quote 12.6 m) include an archive, accessible for maintenance only and a part of the solar roof of the left part of the building. The solar roof of the right part of the building has a quote of 14.41 m, and the solar roof of the archive is at the quote of 15.09 m. The plan dimensions are approximately  $45 \times 19$  m. The masonry infills are made of 40 cm thick tuff blocks and the floors are made of reinforced concrete and hollow tiles having a total thickness of  $25 + 5$  cm. The structure is made of concrete class C25 / 30 reinforced with improved adherence rebars B450C. In particular, the structure is made with  $60 \times 60$  cm pillars on the various floors, connected together by  $60 \times 70$  cm beams and brick and concrete floors with a total thickness of 30 cm consisting of a 5 cm slab. Moreover, at ground floor, at the entrance on the main façade there is a portico characterized by six pillars of  $60 \times 80$  cm. There is

no information regarding the walls of the building, which is about 0,50 m thick, which can be deduced from the plants.

For clearness, in Fig. 4 is shown a photo of the building prospectus and Figs 5, 6, 7, and 8 show the plants of the first floor (similar to the second floor), of the third level (archive and solar roof), of the fourth level (solar roof of the right part of the building) and of the fifth level (solar roof of the archive) with different quotes, the right part (quote 14.41 m) and the left part (15.09 m).

## 3. Experimental tests

The experimental tests on the analyzed buildings have been performed by using the same equipment recently used by the research group (see Diaferio *et al.* 2019, Foti *et al.* 2015, Ivorra *et al.* 2019a, Ivorra *et al.* 2019b) composed by several piezoelectric monoaxial accelerometers (Integrated Circuit Piezo-Electric (ICP), model 393B31, PCB) and the appropriate system of data acquisition. The accelerometers permit to get accelerometers data for low frequency and low acceleration values. They have been mounted, through a threaded pin (as shown in Fig.9(a)), on a cubic-shaped metal element so that they can be arranged orthogonally to each other so that each one measures the acceleration value along the reference axis along which it was placed. The cubic support element is then fixed to the structure at the point to monitor. The data acquisition unit is composed by several modules NI-9230 (Fig. 9(b)), a three-channel control unit,  $12.8 \text{ kS/s/channel}$ ,  $\pm 30 \text{ V}$ , capable of measuring signals from different modules simultaneously and inserted in an opportune DAQ chassis for multiple modules (Chassis cDAQ-9178 till 8 modules). The acquisition system has been programmed by using NI software (Labview) with a sampling frequency of 512 Hz and an acquisition time of 10 minutes for each test. For



(a) accelerometer blocks



(b) acquisition module

Fig. 9 Cubic support element and acquisition module

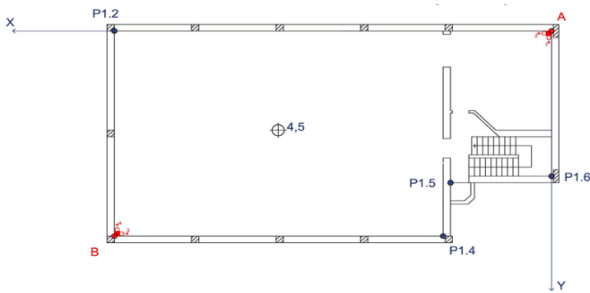


Fig. 10 Positions of accelerometers A and B, quote  $z=4.5$

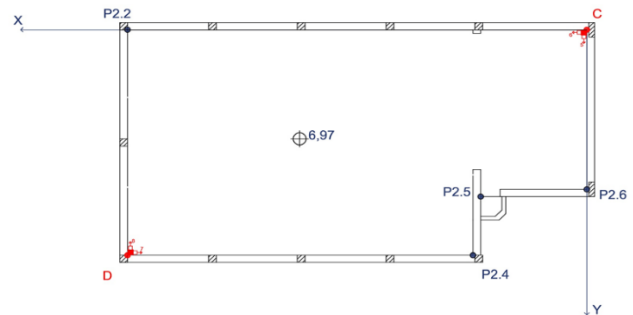


Fig. 11 Positions of accelerometers C and D, quote  $z=6.97$

checking the repeatability of the data at least 3 tests of 10 minutes have been carried out for each structure.

### 3.1 Experimental tests of the fire brigade of Castellaneta

After a preliminary inspection of the structure, in order to understand the real conditions, verify the information previously obtained from the documents and understand where the relevant instruments would have been subsequently applied it was verified that the structure was overall compliant with what is reported in the documentation provided, only on the first floor the vaulted roof was not visible since there was a false ceiling for the lifelines. Despite the false ceiling, it was possible to inspect it inside, finding that it is applied precisely to the vault buttress and, therefore, to the height of 2.47 m.

During the inspection, the points where to apply the blocks with the accelerometers were chosen; the goal was to identify significant accessible points of the structure, in order to obtain a dynamic response that is as realistic as possible. In this regard, 4 points have been identified in which to place 8 accelerometers (2 for each point in orthogonal x, y directions). Two selected points at an altitude of 4.5 m, or at the level of the inter-floor slab, named A and B, and 2 at the level of the begin of vault, or 6.97m (4.5 + 2.47) named C and D. The points are shown in Figs 10 and 11 on the plants with the indication of the considered reference system xy and other points of the structures useful in the following identification analysis. A three-dimensional view of the structure with the indication of the points considered for the analysis at ground floor,

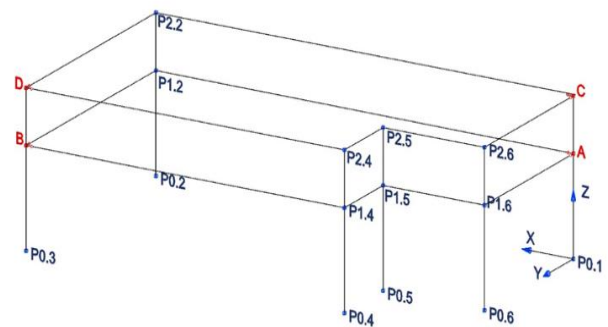


Fig. 12 3D view of the considered points of the structure

intermediate floor and coverage floor, and of the position of accelerometers is shown in Fig.12. In Fig. 13, photos of the 4 accelerometers placed in the points A and C mounted on the structure, highlighted with red circles in Fig. 13(a) and point C zoomed in Fig. 13(b).

### 3.2 Experimental tests of the fire brigade of Castell aneta

In this case 11 points were identified where to place 22 accelerometers (2 for each point in the x, y direction). The points identified with their nomenclature and the reference system xy are shown in the plans of the building in the Figs 14-18. In the same Figs are introduced the names of the other points used for the identification. In Fig.19 a photo of three points (G, H, I at different levels) with the couple of accelerometers installed.

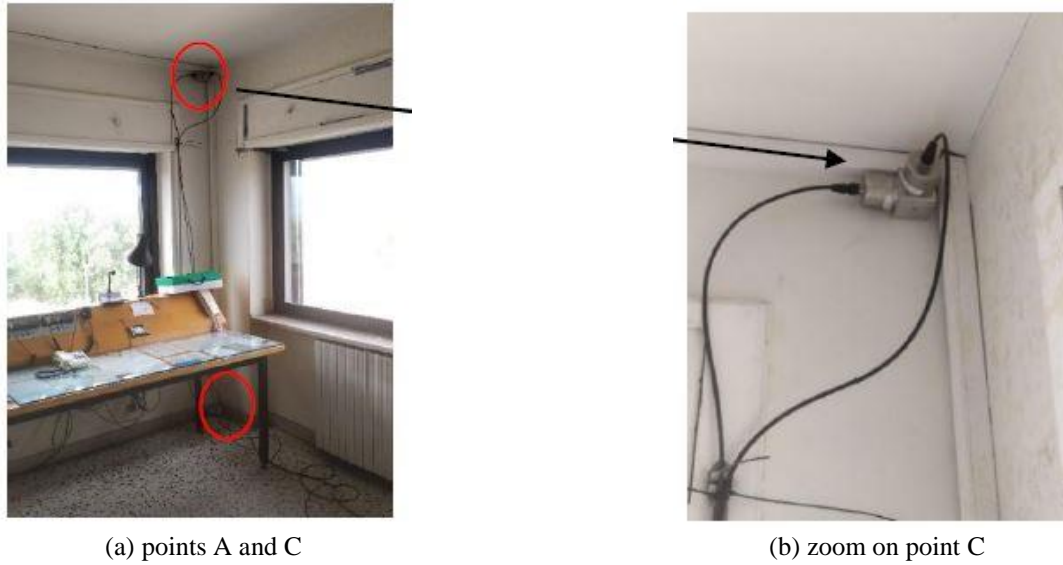


Fig. 13. Photos of the used accelerometers

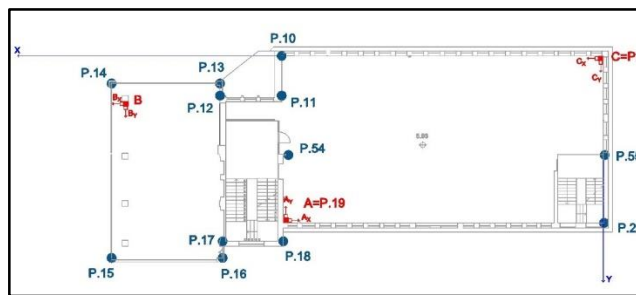


Fig. 14 Positions of accelerometers A, B, C quote  $z=5.93$  m

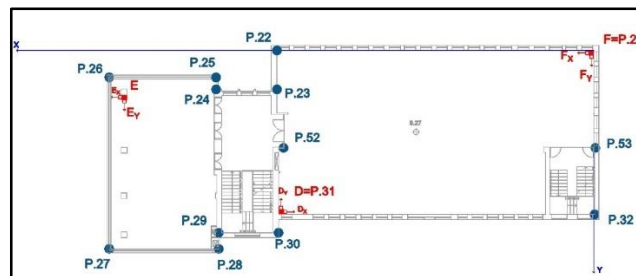


Fig. 15 Positions of accelerometers D, E, F quote  $z=9.27$  m

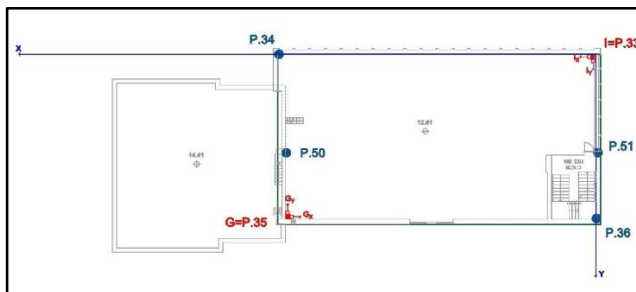


Fig. 16 Positions of accelerometers G, I quote  $z=12.6$  m

#### 4. OMA results

The experimental data carried out from the tests on the two strategic buildings have been carefully preliminary

analyzed for checking eventually accelerometers that had anomalous behaviour during the tests. Then, for each building, three different tests have been analysed with two OMA techniques (Artemis, 2019), one in the frequency

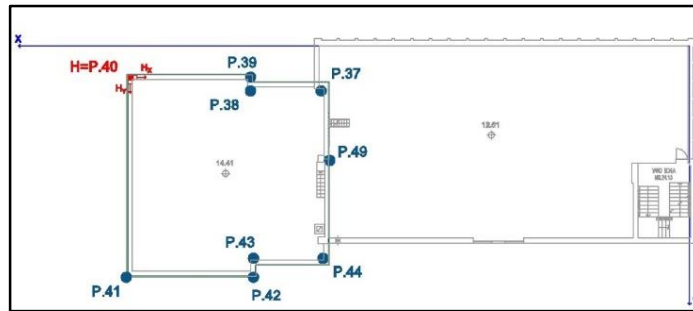


Fig. 17 Position of accelerometers H quote  $z=14.41$  m

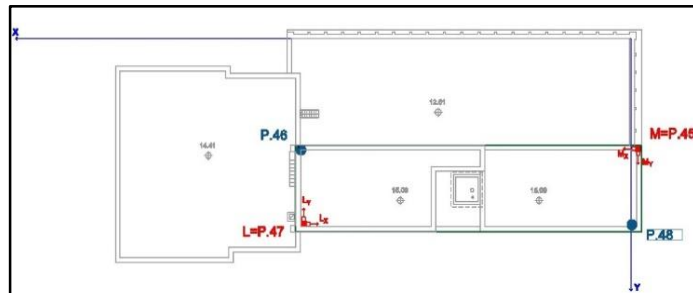


Fig. 18 Positions of accelerometers L, M quote  $z=14.41$  m



(a) point G



(b) point H



(c) point I

Fig. 19 Photo of the used accelerometers

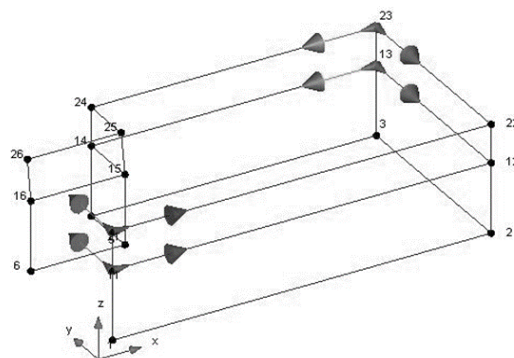


Fig. 20 Geometry and accelerometers positions

domain, the Enhanced Frequency Domain Decomposition (EFDD) method and the second in the time domain, the Crystal-Clear Stochastic Subspace Identification (CC-SSI) method. The repeatability of the identified frequency values with the two techniques and for all the considered tests has permitted to be very confident about the identified

frequencies and modes for both the structures.

#### 4.1 OMA results for the fire brigade of Castellaneta

The preliminary analysis of the 8 accelerometers data for the considered tests did not show anomalies. The

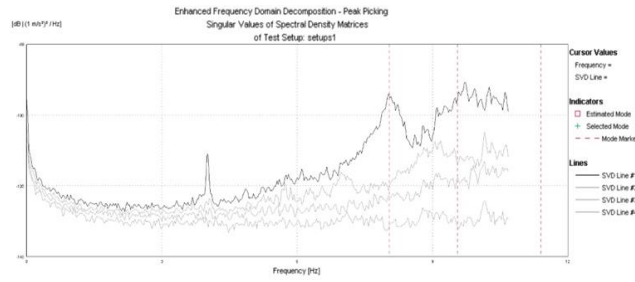


Fig. 21 EFDD identification diagram for Test 1

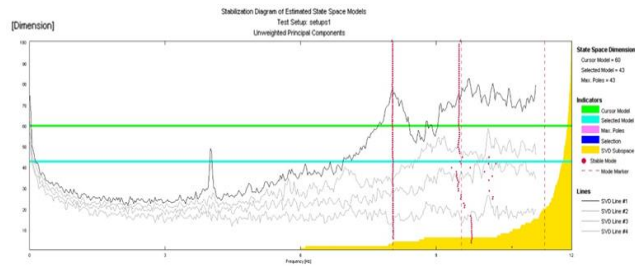


Fig. 22 SSI identification diagram for Test 1

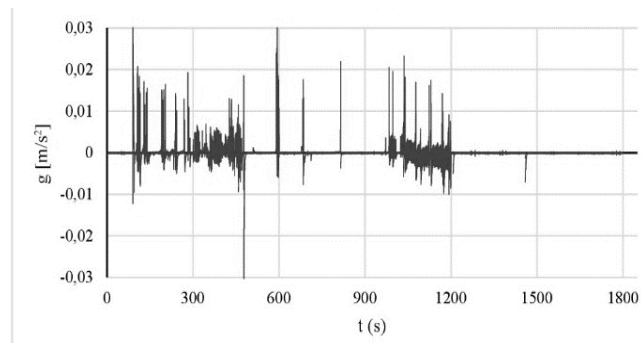


Fig. 23 Accelerometer time history at point F, Test 1

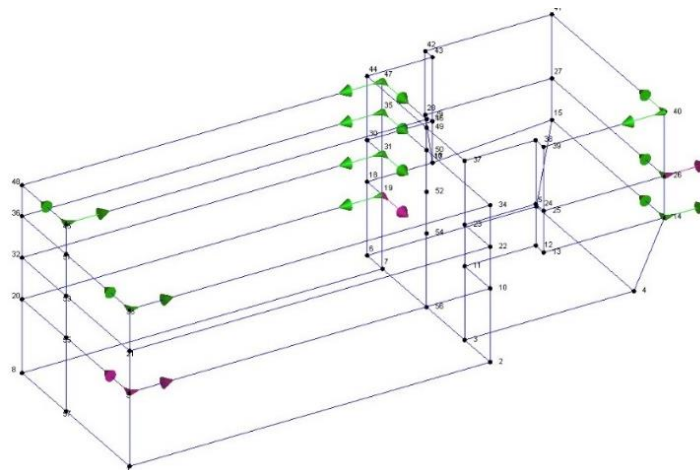


Fig. 24 Geometry and accelerometers positions

Table 1 Identified frequencies [Hz] for Test 1, Test 2, Test 3

Identified frequencies	Test 1	Test 2	Test 3	Mode description
1 <sup>st</sup>	8.06	8.04	8.05	Flexural along x
2 <sup>nd</sup>	9.7	9.55	9.64	Flexural along y
3 <sup>rd</sup>	11.31	11.4	11.37	Torsional

geometry of the structure has been reconstructed for the identification phase with 18 points having the same nomenclature as in Fig. 12. The building geometry used for the analysis with the indication of the accelerometers positions and directions (indicated as arrows) and the reference system xyz is shown in Fig. 20. Three different

Table 2 Identified frequencies [Hz] for Test 1, Test 2, Test 3

Identified frequencies	Test 1	Test 2	Test 3	Mode description
1 <sup>st</sup>	3.61	3.63	3.61	Flexural along x
2 <sup>nd</sup>	3.64	3.65	3.67	Flexural along y
3 <sup>rd</sup>	4.22	4.22	4.21	Torsional

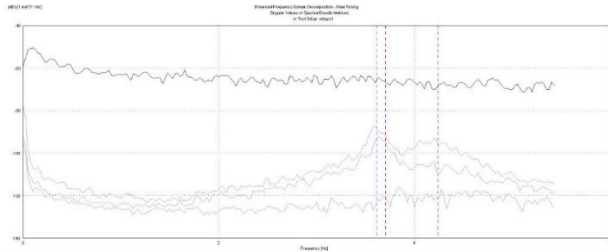
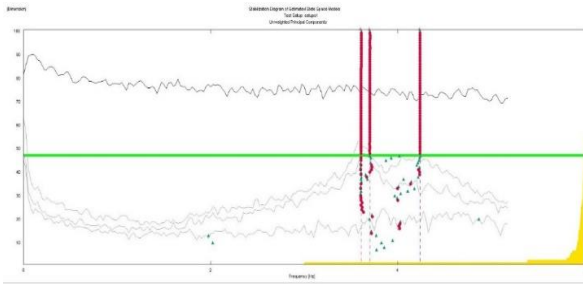


Fig. 25 EFDD identification diagram for Test 1



tests, named Test 1, Test 2 and Test 3, each of them 10 minutes of length with a sampling time of 512 Hz have been analyzed using CC-SSI technique and successfully verified with EFDD. The first 3 identified frequencies and the description of the corresponding modes are summarized in Table 1 and the diagrams of EFDD analysis and CC-SSI analysis for Test 1 are shown in Figs. 21 and 22. It is evident the repeatability of the three identified frequencies on the different tests and with the different techniques ensuring the goodness of the results obtained.

#### 4.2 OMA results for the City Hall of Ginosa

The preliminary analysis of the 22 accelerometers data for the considered tests showed important anomalies for the data carried out from the accelerometers placed in the point F (mainly for one of them). For completeness Fig. 23 reports the time history of the anomalous accelerometer (during Test 1) showing important peaks not registered by any other accelerometer. For this reason, the accelerometers in point F position have not been considered for the identification analysis. The geometric model considered, shown in Fig. 24, depicts the points and the accelerometers location and direction (represented as arrows); in correspondence to point F, that is point 23 in the model in Fig. 24, are not considered accelerometers.

Also, in this case three different tests, Test 1, Test 2 and Test 3, with the same modalities of the Fire Station building have been analyzed using CC-SSI technique and then

successfully verified with EFDD technique. The first three identified frequencies and the description of the corresponding modes are summarized in Table 2 and the diagrams of EFDD analysis and CC-SSI analysis for Test 2 are shown in Figs. 25 and 26. Also, in this case nevertheless the complex profile of the structure, it is evident the repeatability of the three identified frequencies on the different tests and with the different techniques ensuring the goodness of the results so obtained.

## 5. SMAV analysis

The SMAV (Seismic Model from Ambient Vibration) methodology is aimed at evaluating the structural operation of strategic buildings, limited to the occurrence of damage. It is based on the extraction of the experimental modal parameters of the structure (Mori *et al.* 2015, Spina *et al.* 2018). The general objective is to evaluate the ability of strategic buildings, fundamental for the management of emergencies, not to suffer damage such as to compromise their operation within a framework of assessment of the overall capacity of the urban system to satisfy the Limit Condition for the Emergency (CLE) (Bramerini *et al.* 2014). To this end, a Structural Operationality Index (IOPS) for a given seismic action is proposed for the characterization of their vulnerability based on a non-destructive operational modal analysis. Other simple indicators for seismic performances have already been introduced (Tekeli *et al.* 2017) or strategies that considers a probabilistic approach (Song *et al.*, 2017); in the proposed approach, the simplicity of the indicator based on probabilistic approach is coupled with the non-destructivity and simplicity of the necessary experimental tests. In fact the SMAV model (Mori *et al.* 2015, Spina *et al.* 2018) is based on the experimental modal parameters of the building, that is modal frequencies and mode shapes, used to calculate the seismic response of the structure through a dynamic linear analysis that operates by modal superposition. To perform linear dynamic analyzes it is necessary to know the seismic participation coefficient or, alternatively, the seismic mass of each mode of vibration. Necessary, these parameters cannot be obtained experimentally through the OMA, they are obtained numerically by defining a kinematic-inertial model of the building, or Multi Rigid Polygons (MRP). In the MRP model the building is divided into “p” decks above ground, each of which is in turn divided into “n” polygons, which are assumed to have rigid behavior in their own plane and are therefore equipped with three degrees of freedom, i.e. two translations and a rigid rotation around the vertical axis passing through the center of gravity. All the masses of the building, even those that do not lie on the floor of the deck, such as the masses of the vertical load-bearing structures or of the infill, are concentrated in the center of gravity of the polygons, where a mass  $M_x = M_y$  and a moment of polar inertia  $I$  are assigned. The SMAV model allows to calculate the seismic response in all the points of a certain deck, that is, also the points not subject to experimental measurements. The mathematical model also allows to estimate the error committed in the reconstruction of displacements due to the

kinematic hypothesis of rigid polygon, comparing the modal forms originally imported with the reconstructed modal forms, in the same degrees of freedom with the MRP model.

The mass matrix is built by evaluating the translational and rotational masses starting from an analysis of the loads acting on the rigid decks, manually defined when defining the geometries and the volume weights of the structural elements (defining the density of the material). Thus, the mass per unit area is calculated for each polygon that constitutes a horizontal. Once the experimental modal forms are expressed in the rigid degrees of freedom that characterize the kinematic model with rigid polygons, the matrix  $M$  allows to calculate the modal participation coefficients and the corresponding participating masses.

The analysis method consists of:

- Determination of the ways of vibrating of the structure;
- Decoupling of the equations of motion;
- Calculation of the effects of the seismic action for each of the calculated ways of vibrating and combination of these effects.

We can speak of an equivalent linear analysis as the SMAV model takes into account the decrease in natural frequencies as deformation increases (Dunand, 2005, Michel *et al.* 2011) through an iterative procedure based on three limit curves, obtained from a probabilistic analysis, which express the decrease in natural frequencies in function of the maximum average drift, i.e. the maximum displacement of the last deck with respect to the ground, divided by its height  $H$  with respect to the ground. It is named inter-plane drift

To evaluate the decay of the frequencies as the drift changes, considering the variability present in the existing building stock, a “Monte Carlo” type analysis is used for both masonry and reinforced concrete structures, obtaining representative reduction curves uncertainties about the parameters. In the absence of available experimental data, a sample of data is generated where ranges of values are assigned to the parameters necessary to define the model, treating them as random variables having probabilistic distribution. Starting from the generated sample, three curves are obtained, below which respectively 16, 50 and 84% of the samples fall, which define the lower, average and upper limit curve. A first analysis is performed using the building's natural frequencies resulting from the modal identification and the values of accelerations, displacements and inter-floor drifts are calculated for each curve at each point or pair of points. Once the average drift is known, the relative drift is calculated through the frequency decay and a second analysis is carried out using the lowered frequencies, obtaining new drift values. The analysis continues in this way until convergence, generally achieved in less than 10 iterations, in the hypothesis of modal forms invariant with respect to the maximum average drift. For damping, also assumed invariant, the conventional value of 5% is assumed, as required by the NTC2018. The cumulative probability of the maximum drift of the building is obtained by performing three different equivalent linear analyzes, each with reference to one of the three curves described above, which correlate the decrease in frequency

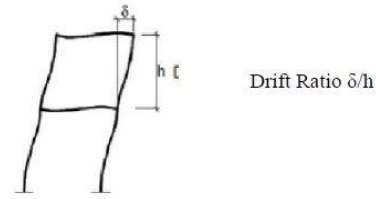


Fig. 27 Graphical visualization of the Interstorey Drift Ratio

to the average drift. The first analysis refers to the average curve, while the other two represent the lower and upper limit curve. Starting from the three maximum drift values thus obtained, for a given seismic input, the cumulative probability function of the maximum drift of the building is constructed, assuming for it a log-normal distribution, which was the most suitable to represent the random interstorey drift variable, following an analysis aimed at comparing the different probability distribution.

The Structural Operating Index (IOPS) consists of a final evaluation of the building based on the assignment of a probabilistic distribution to the “drifts” of the IDR plan (Interstorey Drift Ratio) (depicted in Fig. 27).

It may be considered as the probability that the construction may not be damaged or suffer limited damage, such as to allow its maintenance in operation through the corresponding cumulative probability functions, using the relationship (1):

$$IOPS = P(\delta_{max,SMAV} \leq \delta_{LIM}) \quad (1)$$

The performance level required to meet the emergency limit condition (CLE) is, therefore, that of structural operations, corresponding in the NTC2018 (National Technical Norms, 2018) to the Operating Limit States.

The last data input form concerns seismic input. Data relating to the seismic action can be entered: the analysis can be carried out using a response spectrum, built according to the requirements of the Technical Standards for Construction, or through the import of an ad hoc spectrum). It is also possible to conduct an analysis in the time domain by importing accelerograms: in this case the algorithm will return the time history of accelerations and displacements in each of the points of the structure defined in the previous panel. In this case, an elastic response spectrum defined according to NTC2018 was imported and the SMAV analysis was conducted with elastic response spectrum for the Damage Limit State (SLD), with reference to the use class IV (accelerogram shown in Fig. 28). The verification of the structural operation, corresponding to the SLD, is carried out in terms of displacements, a seismic action with a probability of exceeding 63% in 100 years corresponding to a return period of 100 years. The assessment linked to this seismic action responds to what is prescribed by the NTC2018 for the verification of strategic buildings at the SLD.

The seismic action is expressed without considering any structure factor, using the elastic response spectrum for both actions. In relation to this seismic action described, the  $IOPS_{100}$  is calculated. The methodology provides an assessment of the structural operation of the strategic

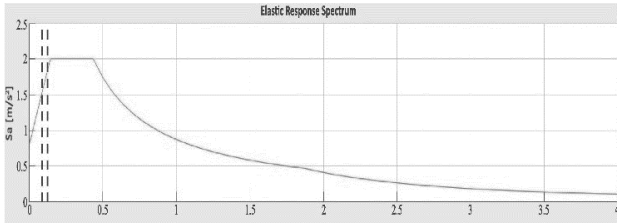


Fig. 28 Elastic response spectrum used for SLD analyses

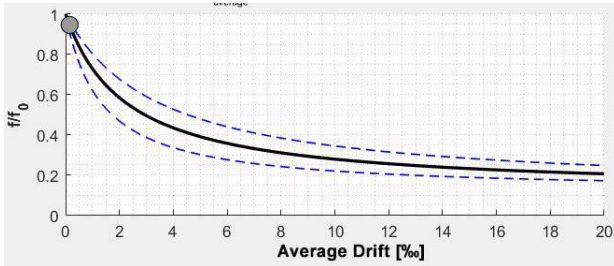


Fig. 29 Decline curve from Test 1 data

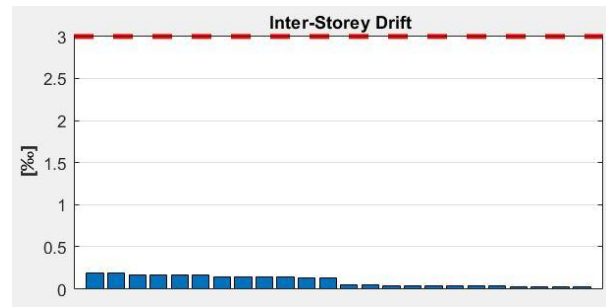


Fig. 30 Inter-Storey drift values for SLD from Test 1 data

buildings that are part of the emergency management system.

### 5.1 SMAV results for the fire brigade of Castellaneta

The structure of the building is inserted in the SMAV procedure by introducing the points defining the first and second floor, the six point for each plane depicted in Fig. 12. Moreover, as regards the floors, a thickness of 30 cm and a density equal to 12 kN / m<sup>3</sup> has been defined; for load bearing masonry, on the other hand, a thickness of 40 cm and a density equal to 22 kN / m<sup>3</sup> has been considered. Finally, considering the mode shape residues for each considered frequency (the 3 identified frequency) and the seismic input (spectrum in Fig. 28), it is possible to calculate, through the assumed rigid behavior of each plane, the time history of the accelerations and displacements in each of all the defined points of the structure (six points for first floor, six for second floor, totally 12 points), the inter plane drift and the decline curve as previously described.

Considering the experimental data carried out from Test 1, the decline curve is shown in Fig. 29. Moreover the Inter-storey drift (express in percentage), the maximum accelerations and maximum displacements for the 12 points of the building (considering for each of them x direction and y direction, so totally 24 values analyzed) are shown in Figs 30, 31 and 32, and the abscissa points components are ordered following the Inter-Storey drift values.

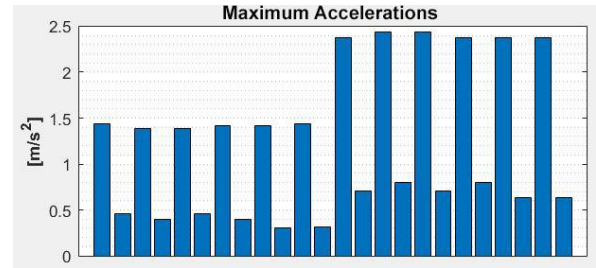


Fig. 31 Maximum accelerations for SLD from Test 1 data

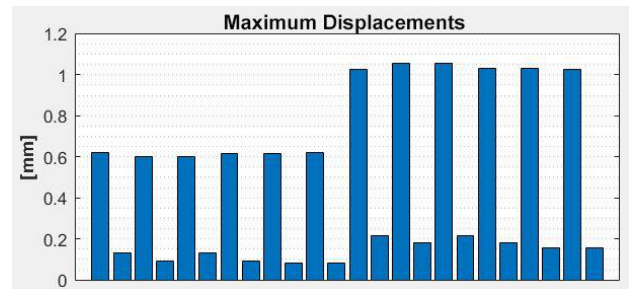


Fig. 32 Maximum displacements for SLD from Test 1 data

Table 3. SMAV results for the SLD analysis

Parameter name	Test 1	Test 2	Test 3
Maximum drift [%]	0.18	0.19	0.20
Shift of decline curve [%]	5.38	5.49	5.46
Maximum displacement $\delta_{MAX}$ [mm]	1.06	1.09	1.09
Maximum acceleration [m/s <sup>2</sup> ]	2.4	2.5	2.5
IOPS <sub>100</sub>	7.07	6.88	6.88

From the data shown in Fig. 30, it is possible to estimate a maximum drift of 0.18%, that means, on the median curve of the decline curve, a shift of 5.38% (the corresponding point is a circle in Fig. 29), and a maximum displacement  $\delta_{MAX}$  of 1.06 mm (data in Fig. 32).

Following the technical norms (NTC,2018), the value of  $\delta_{LIM}$  that appears in (1) may be determined by (2) where h is the maximum interplane distance, equal in this case to 4500 mm. Finally, it is possible to calculate the IOPS<sub>100</sub> by using (3).

$$\delta_{LIM} = \frac{2}{3} \cdot 0.0025 \cdot h = 7.5 \text{ mm} \quad (2)$$

$$IOPS_{100} = \frac{\delta_{LIM}}{\delta_{MAX}} \quad (3)$$

For the considered case IOPS<sub>100</sub>= 7.07 that is a value of absolutely safety for the strategic building considered and there is a wide margin of safety for the considered building. Similar results were carried out by using the experimental identification data of the other tests (Test 2 and Test 3); in Table 3 a general summary of all the results obtained applying the SMAV procedure with reference to the identified modal data referred to Test 1, Test 2 and Test 3.

The excellent repeatability for the different tests increases the affordability of the analysis and permit to

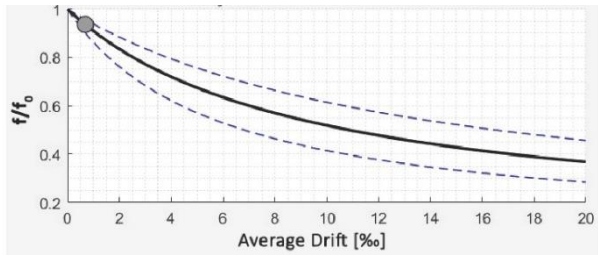


Fig.33 Decline curve from Test 1 data

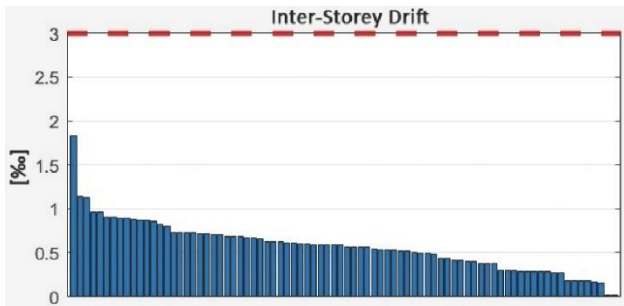


Fig. 34 Inter-Storey drift values for SLD from Test 1 data

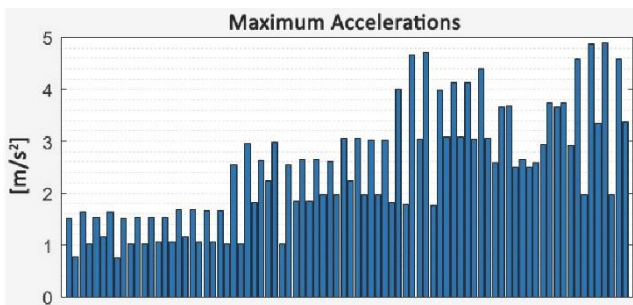


Fig.35 Maximum accelerations for SLD from Test 1 data

extract important and positive information about the operativity of a strategic building.

## 5.2 SMAV results for the City Hall of Ginosa

The structure of this building is inserted in the SMAV procedure similarly at the previous building. In this case five floors have been inserted as rigid planes with total of 41 points necessary to describes the 5 decks from first to fifth floor (extracted from the 57 points depicted in Figs. 14 - 18 neglecting the 10 points at ground floor and the inner points in the other five floors). Moreover, as regards the floors, a thickness of 30 cm and a density equal to 20 kN /m<sup>3</sup> has been considered for first and second floor and a density of 17 kN /m<sup>3</sup> for the upper floors, considering the information on the plants. The contribute of the walls has been neglected. Finally, considering the mode shape residues for each considered frequency (the 3 identified frequencies) and the seismic input (spectrum in Fig. 28), it is possible to calculate, through the assumed rigid behavior of each plane, the accelerations and displacements in each of all the defined 41 points of the five decks of the structure, the inter plane drift and the decline curve as previously described. Similarly, to the analysis shown in the previous paragraph, also in this case the decline curve is

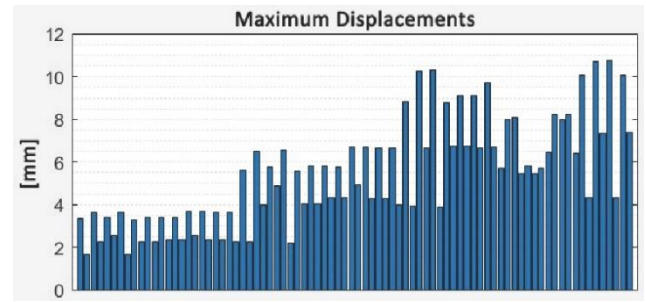


Fig.36 Maximum displacements for SLD from Test 1 data

Table 4. SMAV results for the SLD analysis

Parameter name	Test 1	Test 2	Test 3
Maximum drift [%]	1.83	1.04	0.9
Shift of decline curve [%]	6	4.57	1.29
Maximum displacement $\delta_{MAX}$ [mm]	10.8	10.8	5.97
Maximum acceleration [m/s <sup>2</sup> ]	4.9	4.9	2.9
IOPS <sub>100</sub>	1.83	1.83	3.3

shown in Fig. 33 considering the experimental data carried out from Test 1. Moreover the Inter-storey drift, the maximum accelerations and maximum displacements for the 41 points (considering for each of them x direction and y direction, so totally 82 values analyzed) are shown in Figs 34, 35 and 36, and the abscissa points components are ordered following the Inter-Storey drift values. From the data shown in Fig. 34, it is possible to estimate a maximum drift of about 1.83%, that means, on the median curve of the decline curve, a shift of 6% (the corresponding point is a circle in Fig. 33), and a maximum displacement  $\delta_{MAX}$  of 10.8 mm (data in Fig. 36). The maximum displacement  $\delta_{LIM}$  required by law (NTC-2018), for buildings reinforced concrete buildings with fragile infill, it is given by (4), where, in this case, the interplane value h is 5.93 m.

$$\delta_{LIM} = \frac{2}{3} \cdot 0.005 \cdot h = 19.8 \text{ mm} \quad (4)$$

Applying Eq. (3) it is possible to calculate IOPS<sub>100</sub>=1.83 that, also in this case is a value that guarantee that the strategic building has a good structural operativity, although not so high as the other building analyzed. Anyway, considering the analysis based on the other 2 experimental tests (Test 3 and Test 4) the results, summarized for all the cases in Table 4, are very close and slightly better confirming the classification related to the operativity index.

## 6. Conclusions

This research has the objective of identifying the dynamic characteristics of two buildings of strategic importance, through dynamic identification techniques by

environmental input of the “OMA” type and the installation, on the structural elements, of highly sensitive sensors able to acquire the vibrations of the supporting structure. The advantage of this technique was inherent to the possibility to operate without interrupting the activities within the structure, which cannot be subject to interruptions in the monitoring activity. After the experimental evaluation of the dynamic characteristics of the structure, the structural operating index (IOPS) was calculated by means of SMAV methodology, for the characterization of the operativity of these strategic structures. In addition to the structural operating index it has been possible to extract also the maximum floor displacements that could occur in the event of an earthquake, of which the response spectrum for SLD has been considered. It was found that both the analyzed structures are operational, despite their important structural differences and states.

The advantages obtained from the analysis here developed are related to the speed of execution with the least invasiveness, the ease of implementation of the algorithm, the precision of the results, as it is based on the experimental data obtained by OMA, the ability to be able to model structurally complex buildings in a simple way. The methodology, at present, shows some critical issues related to the use of limit drift values and general frequency reduction curves, and to the essentially linear character of the SMAV model.

In conclusion, this study allows us to understand the importance, for strategic buildings, of carrying out an in-depth study on their dynamic characteristics and the operational status. As a consequence, it will be possible to intervene promptly, since, in case of exceptional events such as the earthquake, these buildings have a “strategic” role of control, monitoring and intervention, so it is not possible in such situations to interrupt the activity or, even worse, to suffer serious structural damage or collapses.

## Acknowledgments

This work was carried out as part of a research agreement among Polytechnic University of Bari (coordinator Prof. Dora Foti), University of Basilicata (coordinator Prof. Felice Ponzio), and the Institute of Environmental Geology and Geoengineering of the National Research Council (coordinator Federico Mori). Research activities were performed in the framework of the project “PO Governance 2014-2020 project on the reduction of seismic, volcanic and hydrogeological risk for civil protection purposes – CIG 6980737E65 – CUP J59G16000160006”, funded by the Presidency of the Council of Ministers Department of Civil Protection.

## References

Acunzo, G., Fiorini, N., Mori, F. and Spina, D. (2015), “VaSCOSMAV: il software sviluppato per l’applicazione della metodologia SMAV”, The Proceedings of the XVI Conference ANIDIS, September.

Acunzo, G., Fiorini N., Mori F. and Spina, D. (2018), “Modal

mass estimation from ambient vibrations measurement: A method for civil buildings”, *Mech. Syst. Signal Processing*, **98**, 580-593. <https://doi.org/10.1016/j.ymssp.2017.05.014>.

ARTEMIS (2019), “Ambient Response Testing and Modal Identification Software ARTEMIS Extractor Pro 5.3. Structural Vibration Solution A/S Aalborg East”, Denmark. [www.svibs.com](http://www.svibs.com)

Bramerini, F. and Castenetto, S. (2014) “Manuale per l’analisi della Condizione Limite per l’Emergenza (CLE) dell’insediamento urbano, Versione 2.0”, Betmultimedia, Roma, Italy.

Bru, D., Ivorra, S., Baeza, F.J., Reynau, R. and Foti, D. (2015), “OMA Dynamic Identification of a Masonry Chimney with Severe Cracking Condition”, *The 6th International Operational Modal Analysis Conference, Proceedings*.

Diaferio, M., Foti, D., Ivorra, S., Giannoccaro, N.I., Notarangelo, G. and Vitti, M. (2019), “Monitoring and structural identification of a “Star-shaped” reinforced concrete bell tower”, *The 8th IOMAC - International Operational Modal Analysis Conference, Proceedings*, 47-54.

Dunand, F. (2005), “Relevance of seismic noise for dynamic characterization using seismic and diagnosis of civil engineering structures”, Ph. D Dissertation, University Joseph Fourier, Grenoble.

Foti, D., Diaferio, M., Giannoccaro N.I. and Mongelli M. (2012), “Ambient vibration testing, dynamic identification and model updating of a historic tower” *NDT. E. Int.*, **47**, 88-95. <https://doi.org/10.1016/j.ndteint.2011.11.009>.

Foti, D., Giannoccaro, N.I., Diaferio, M. and Ivorra, S. (2015), “Structural identification and numerical models for slender historical structures” in Handbook of Research on Seismic Assessment and Rehabilitation of Historic Structures, 674-703, IGI Global, Hershey, Pennsylvania, U.S.A.

Ivorra, S., Foti, D., Gallo, V., Vacca, V. and Bru, D. (2019a), “Bell’s dynamic interaction on a singular concrete bell tower: A case of Study”, *Eng. Struct.*, **183**, 965-975. <https://doi.org/10.1016/j.engstruct.2019.01.071>.

Ivorra, S., Giannoccaro, N.I. and Foti, D. (2019b), “Simple model for predicting the vibration transmission of a squat masonry tower by base forced vibrations”, *Struct. Control Health Monit.*, **26**(6), 1-21. <https://doi.org/10.1002/stc.2360>.

Mazza, F. (2019a) “A plastic-damage hysteretic model to reproduce strength stiffness degradation.” *Bulletin of Earthquake Engineering*, **17**, 3517-3544.

Mazza, F. (2019b), “A simplified retrofitting method based on seismic damage of a SDOF system equivalent to a damped braced building”, *Eng. Struct.*, **200**, 109712. <https://doi.org/10.1016/j.engstruct.2019.109712>.

Mazza, F. (2019c), “In-plane-out-of-plane non-linear model of masonry infills in the seismic analysis of r.c.-framed buildings”, *Earthq. Eng. Struct. Dyn.* **48**(4), 432-453. <https://doi.org/10.1002/eqe.3143>.

Michel, C., Zapico, B., Lestuzzi, P., Molina, F.J. and Weber, F. (2011), “Quantification of fundamental frequency drop for unreinforced masonry buildings from dynamic tests”, *Earthq. Eng. Struct. Dyn.*, **40**(11), 1283-1296. <https://doi.org/10.1002/eqe.1088>.

Mori, F. and Spina, D. (2015), “Vulnerability assessment of buildings based on ambient vibrations measurements”, *Struct. Monit. Maintenance*, **2**(2), 115-132. <https://doi.org/10.12989/smm.2015.2.2.115>

Norme Tecniche per le Costruzioni (NTC-2018), “D.M. 17 Gennaio 2018, Gazzetta Ufficiale 20 Febbraio 2018, Rome, Italy.

Peeters B. and De Roeck, G. (2001), “Stochastic system identification for operational modal analysis: a review”, *J. Dyn Syst. Meas. Control*, **123**, 659-667.

<https://doi.org/10.1115/1.1410370>.

- Ranieri, C. and Fabbrocino, G. (2014), “Operational modal analysis of civil engineering structures: an introduction and guide for applications”, Springer, Berlin, Germany.
- Reynders, E. (2012), “System identification methods for (operational) modal analysis: review and comparison”, *Archives Comput. Meth. Eng.*, **19**, 51-124. <https://doi.org/10.1007/s11831-012-9069-x>.
- Spina, D., Acunzo, G., Fiorini, N. and Dolce, M. (2019), “A probabilistic simplified seismic model of masonry buildings based on ambient vibrations”, *Bull. Earthq. Eng.*, **17**(2), 985-1007. <https://doi.org/10.1007/s10518-018-0481-y>.
- Tekeli H., Dilmac H., Demir, F., Gencoglu, M. and Guler, K. (2017), “Shear stress indicator to predict seismic performance of residential RC buildings”, *Comput. Concrete*, **19**(3), 283-291. <https://doi.org/10.12989/cac.2017.19.3.283>.

AT